ISSN 1674-1056
http://cpb.iphy.ac.cn
http://iopscience.iop.org/cpb
中国物理 B
Chinese Physics
中国物理 Chinese Physics B

First-principles study of oxygen adsorbed on Au-doped RuO_2 (110) surface

Ji Zhang(张季)[1], De-Ming Zhang(张德明)[1,2]
Citation: Chin. Phys. B . 2019, 28(11): 116107 . **doi:** 10.1088/1674-1056/ab4cdc
Journal homepage: http://cpb.iphy.ac.cn; http://iopscience.iop.org/cpb

What follows is a list of articles you may be interested in

Geoscience material structures prediction via CALYPSO methodology

Andreas Hermann
Chin. Phys. B . 2019, 28(10): 106107 . **doi:** 10.1088/1674-1056/ab43bc

Structural and electronic properties of transition-metal chalcogenides Mo_5S_4 nanowires

Ming-Shuai Qiu(邱明帅), Huai-Hong Guo(郭怀红), Ye Zhang(张也), Bao-Juan Dong(董宝娟), Sajjad Ali(阿里.萨贾德), Teng Yang(杨腾)
Chin. Phys. B . 2019, 28(10): 106103 . **doi:** 10.1088/1674-1056/ab3f9a

Impeding anion exchange to improve composition stability of $CsPbX_3$ (X=Cl, Br) nanocrystals through facilely fabricated Cs_4PbX_6 shell

Zhaohui Shen(申朝晖), Pengjie Song(宋鹏杰), Bo Qiao(乔泊), Jingyue Cao(曹靖玥), Qiongyu Bai(白琼宇), Dandan Song(宋丹丹), Zheng Xu(徐征), Suling Zhao(赵谡玲), Gaoqian Zhang(张高倩), Yuanjun Wu(吴元均)
Chin. Phys. B . 2019, 28(8): 086102 . **doi:** 10.1088/1674-1056/28/8/086102

Micron-sized diamond particles containing Ge-V and Si-V color centers

Hang-Cheng Zhang(章航程), Cheng-Ke Chen(陈成克), Ying-Shuang Mei(梅盈爽), Xiao Li(李晓), Mei-Yan Jiang(蒋梅燕), Xiao-Jun Hu(胡晓君)
Chin. Phys. B . 2019, 28(7): 076103 . **doi:** 10.1088/1674-1056/28/7/076103

Control on β conformation of poly(9,9-di-n-octylfluorene) via solvent annealing

Zhi Chao Zhang(张志超), Bing Yue Zhang(张丙悦), Yu Yan Weng(翁雨燕), Tian Hui Zhang(张天辉)
Chin. Phys. B . 2019, 28(7): 076101 . **doi:** 10.1088/1674-1056/28/7/076101

First-principles study of oxygen adsorbed on Au-doped RuO_2 (110) surface*

Ji Zhang(张季)[1,†] and De-Ming Zhang(张德明)[1,2]

[1] *An Hui Xin Hua University, Hefei* 230088, *China*

[2] *Anhui Institute of Optics and Fine Mechanics, Chinese Academy of Sciences, Hefei* 230031, *China*

(Received 23 August 2019; revised manuscript received 8 October 2019; published online 30 October 2019)

Density functional theory calculations are carried out to identify various configurations of oxygen molecules adsorbed on the Au-doped RuO_2 (110) surface. The binding energy calculations indicate that O_2 molecules are chemically adsorbed on the coordinatively unsaturated Ru (Ru_{cus}) sites and the bridge oxygen vacancies on the Au sites. Transition state calculations show that O* can exist on the Ru_{cus} site by O_2^* dissociation and diffusion. The calculations of the reaction path of CO indicate that the reaction energy barrier of CO adsorbed on Au with lattice oxygen decreases to 0.28 eV and requires less energy than that on the undoped structure.

Keywords: CO, metal oxides, density functional theory, ruthenium oxide, O_2 adsoption

PACS: 61.66.Dk, 61.72.J–, 61.72.Bb, 61.72.uj **DOI:** 10.1088/1674-1056/ab4cdc

1. Introduction

The physical and chemical properties of transition metal oxides are of great interest and importance for efficiently using catalysis, electrochemistry, and gas sensors. Because the surfaces of these oxides perform well compared with the bulk state, the important goal in such studies is to reveal the surface functionality, especially their interaction with a gas phase species on anatomic scale.[1,2]

In recent years, ruthenium dioxide (RuO_2) has become a popular and convenient model system for investigating catalytic reactions. And CO oxidation has attracted much attention because it plays an important role in solving the exhaust gas issues generated from auto-mobiles and industries. In CO oxidation, the surface of metallic Ru is inactive, but after being highly exposed to O_2, it displays excellent performance due to the formation of a RuO_2 (110) film.[3–6] A Mars–van Krevelen mechanism and a Langmuir–Hinshelwood model were successively proposed for the explaining of the CO catalytic oxidation on the chemical surface.[7,8]In the Mars–van Krevelen model, reductants react with metal oxide lattice oxygen, and then the dissociative adsorption of O_2 fills the resulting oxygen vacancies. The Langmuir–Hinshelwood model suggests that CO combines with dissociated O* into CO_2. Therefore, O_2 adsorption and dissociation are important processes for catalytic reactivity.[9,10] Recent studies have experimentally and theoretically reported that oxygen molecules are adsorbed on the stoichiometric RuO_2 (110) surface.[11,12] On the other hand, to improve the properties of a catalyst, an effective strategy is to modify the metal oxides with other metal elements. For example, the (111) surface of ceria can be made reactive to CO oxidation by doping the surface with Au theoretically.[13] Because doped gold atoms become gold ions which play an important role in determining the CO catalytic oxidation, gold becomes a significant doping element. Therefore, it is interesting to study the oxygen adsorption and CO oxidation on Au-doped RuO_2 (110) surface.

In this study, O_2 adsorption, dissociation, and diffusion on the Au-doped Ru (110) surface are investigated by using density functional theory. First, the optimized configurations of molecular O_2 adsorbed on the Au-doped RuO_2 (110) surface are obtained. Then the adsorption energy and dissociation energy barrier are calculated. The reaction paths of CO adsorbed onto Au with the O* atom are also determined.

2. Computational method

Calculations based on the density functional theory (DFT) were analyzed in the generalized gradient approximation (GGA)[14] by using the Perdew–Burke–Emzerhof function for correlation energy. Plane-wave basis functions were included with a kinetic energy cutoff of 450 eV. The calculations were carried out by using the Brillouim zone sampled with $4 \times 4 \times 6$ and $2 \times 2 \times 1$ Monkhorst–Pack mesh k-points grid for bulk RuO_2 and surface calculations, respectively. The structures were relaxed by using the BFGS algorithm until the forces on all atoms were < 0.02 eV·Å^{-1}. The first-principles calculations were performed by using the Cambridge Sequential Total Energy Package (CASTEP) code.[15]

Figure 1(a) shows the ball-and-stick model for the stoichiometric RuO_2 (110) surface. In the bulk RuO_2, there are six-fold coordinated Ru atoms and three-fold coordinated

*Project supported by the Natural Science Foundation of Anhui Province, China (Grant Nos. KJ2018A0588 and KJ2019A0879).

†Corresponding author. E-mail: coolfall123@126.com

© 2019 Chinese Physical Society and IOP Publishing Ltd

O atoms. However, two types of Ru atoms exist on the RuO_2 (110) surface: one is the type of Ru atom, coordinatively unsaturated Ru_{cus}, which has a five-fold coordination and is connected by a three-fold coordinated oxygen O_{3f}, and the other is the type of Ru atom, Ru_{br}, which has a six-fold coordination and is linked by a two-fold coordinated bridging oxygen O_{br}. Because the oxygen-binding energy is insensitive to slab thickness,[16] two $(RuO_2)_4$ layer slabs were used for the calculations. The slabs were separated by a 15-Å vacuum in the *c*-axis direction. In the present study, one of the Ru_{cus} atoms was replaced by one Au atom as illustrated in Fig. 1(b).

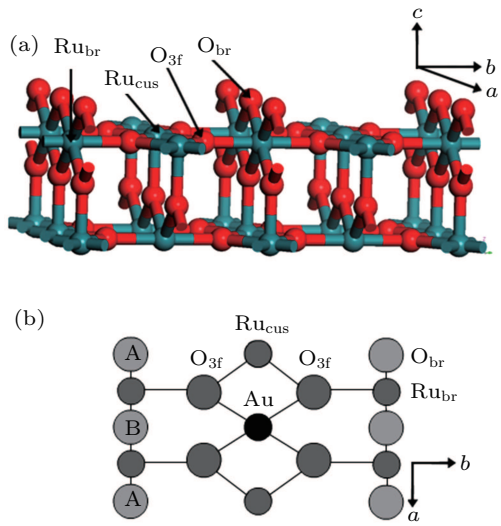


Fig. 1. (a) Structure of RuO_2 (001) surface, showing ball-and-stick representation of stoichiometric RuO_2 (001) surface with red ball representing O atom and cyan balls denoting ruthenium. (b) Top-view of Au-doped RuO_2 (001) surface.

Oxygen dissociation and diffusion barriers were calculated by using the Climbing Image Nudged Elastic Band (CI-NEB) method.[17,18] Five intermediate images were generated between the geometry-optimized initial and final state by linear interpolation. Minimum energy reaction paths were obtained by simultaneously relaxing each image. Vibrational frequencies were calculated through the diagonalization of the Hessian matrix by displacing the atoms by 0.01 Å from their equilibrium positions. The adsorption energy of molecular O_2, the oxygen vacancy formation energy, and the charge density difference were calculated below.

The adsorption energy was evaluated from

$$E_{ad} = E_{mol+surf} - (E_{surf} + E_{mol)}), \quad (1)$$

where $E_{mod+surf}$ represents the total energy of the surface combined with the adsorption molecules, E_{surf} is the total energy of the substrate, and E_{mol} is the total energy of molecules in the gas phase.

The oxygen vacancy formation is described by the reaction $Ru_{1-x}Au_xO_2 \rightarrow Ru_{1-x}Au_xO_{2-\delta} + \frac{1}{2}O_2$.[19] The oxygen vacancy formation energy E_f, was computed from the following equation

$$E_f = E(Ru_{1-x}Au_xO_{2-\delta}) + \frac{1}{2}E(O_2) - E(Ru_{1-x}Au_xO_2), \quad (2)$$

where $E(Ru_{1-x}Au_xO_{2-\delta})$ indicates that the energy of the bulk or $Ru_{1-x}Au_xO_2$ surface, $E(O_2)$ is the energy of gas-phase O_2, and $E(Ru_{1-x}Au_xO_2)$ is the energy of the bulk or surface in the presence of one oxygen vacancy.

The charge density difference ρ_{diff} was obtained from the following expression

$$\rho_{diff} = \rho_{mol+surf} - \rho_{surf} - \rho_{mol}, \quad (3)$$

where $\rho_{mol+surf}$ is the charge density of the adsorbed species on the surface, and ρ_{surf} and ρ_{mol} are the charge densities of the bare surface and the adsorbate, respectively.

3. Results and discussion

3.1. Au-doped $Ru_{0.875}Au_{0.125}O_2$ bulk and surface

RuO_2 crystallizes into a rutile structure with lattice parameters *a* and *c*. To ensure the reliability of the computational results, the bulk lattice constants are predicted and compared with the experimental value. The calculated lattice parameters of the pure RuO_2 are $a = 4.53$ Å and $c = 3.13$ Å, which accord with the results of Sun ($a = 4.52$ Å and $c = 3.13$ Å) obtained through a DFT–GGA pseudopotential study.[20] The theoretical values are similar to the experimental values of 4.492 and 3.306.[21,22] The geometries of stoichiometric and reduced-bulk Au-doped RuO_2 are optimized until the external and internal degree of freedom can relax to the force and stress vanished in the bulk calculations. The lattice constants change after the Au atoms have been doped into the bulk RuO_2, the predicted lattice constants of bulk 12.5% Au-doped RuO_2 are $a = 4.58$ Å and $c = 3.20$ Å, which are slightly larger than those of pure RuO_2 because of larger radius of the Au atom. The optimized $Ru_{0.875}Au_{0.125}O_2$ presents geometric distortion with an average length of the Ru–O bonds, 1.988 Å, while that of Au–O bonds is 2.163 Å. The RuO_2 (110) surface that is built below will use these lattice constants.

The relaxed structure of the Au-doped RuO_2 (110) surface in which one Ru atom is replaced by one Au atom is shown in Fig. 1(b). The bond length between Ru-cus and the O atom below it decreases from 1.962 Å in the bulk to 1.865 Å, which are similar to the values calculated by Hong *et al.*.[23] On the contrary, the bond-length between Au-cus and the O atom below it increases from 2.049 Å in the bulk to 2.331 Å. Therefore, the Au atom is located at the position above the plane with the Ru-cus and O_{3f}.

3.2. Structures of molecular O_2 adsorption

As is well known, O_2 can bind to the transition metal center. In the present study, there are four sites for O_2 adsorption: Ru_{cus}, Au, and O vacancies A and B as shown in Fig. 1(b).

The A site is formed by the vacancy of O_{br} near Ru_{cus}, and the B site is related to the vacancy of O_{br} near the Au atom on the surface. Moreover, the formation energy E_f of the oxygen vacancy is calculated. The O_{br} vacancy on the A site has much smaller formation energy ($E_{fA} = 2.41$ eV) than the undoped RuO_2 (110) surface (2.89 eV), indicating that the O vacancy formation is very much facilitated by Au doping. However, the formation energy for the B site ($E_{fA} = 3.06$ eV) is bigger than that in the undoped case. Therefore, the Au dopant may make the oxygen vacancy formed easier at A site than at B site.

Figure 2 illustrates the DFT-optimized O_2^* bound on the Au-doped RuO_2 (110) surface and density for O_2^* adsorbed at the Ru_{cus} and the Au sites. Binding energy values, O–O bond lengths, Bader charges, and O–O stretching frequencies are summarized in Table 1. First, we consider that O_2^* binds at a single Ru_{cus} site in a bent fashion. There are two configurations in this case. The first situation is that O_2^* is adsorbed vertically on one Ru_{cus} across the coordinatively unsaturated row with Ru–O–O at an angle of approximately 122.8°, and the O–O bond length is 1.284 Å, slightly greater than the O–O bond length of gas-phase molecular O_2. The O–O stretching vibrational frequency is 1229.4 cm^{-1} red-shifted by about 352 cm^{-1} from molecular O_2.[24] The Bader charge analysis shows a 0.22-e^- charge transfer from the Ru_{cus} cation to the O_2^* . The charge transfer is illustrated in the density plot marked as the blue area between O and Ru atoms. These features are all consistent with those of a superoxo-like O_2^- which is characterized by vibrational frequencies near 1140 cm^{-1} and O–O bond lengths of 1.33 Å.[25]

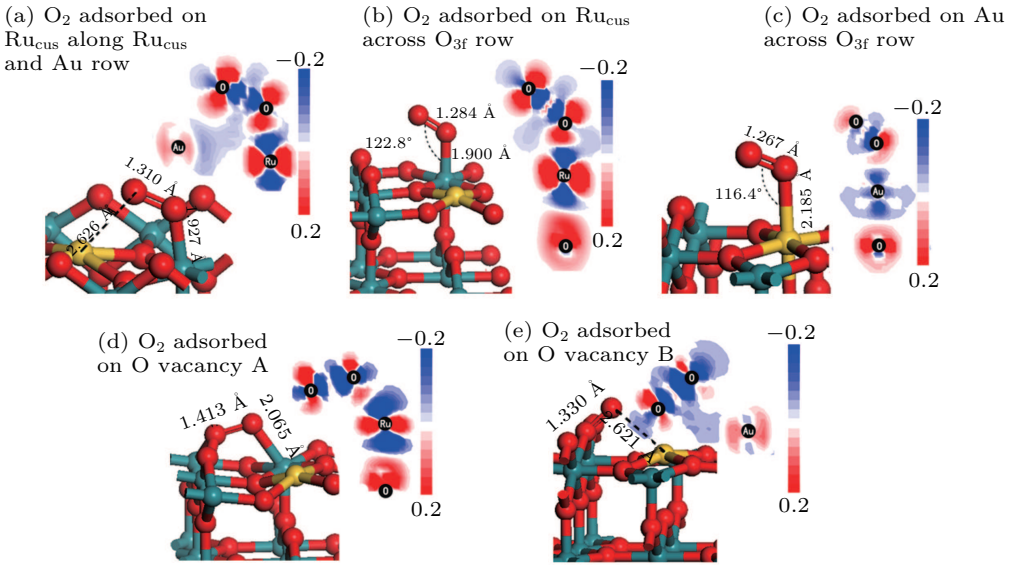


Fig. 2. Representative configurations and charge density differences of molecular oxygen adsorption involving a br vacancy, cus and Au sites.

Table 1. Values of adsorption energy (ΔE_{O_2}), bond length (d_{O-O}), Bader charge of O_2 ($Q^*_{O_2}$), and O–O stretching vibrational frequency (ν).

Fig. 2	ΔE_{O_2}/eV	d_{O-O}/Å	$Q^*_{O_2}$	ν/cm^{-1}
(a)	–1.78	1.31	–0.40	1165.8
(b)	–1.42	1.28	–0.22	1229.4
(c)	–0.44	1.26	–0.29	1317.7
(d)	–7.45	1.41	–0.77	740.7
(e)	–6.98	1.33	–0.62	1078.7

According to Wang *et al.*'s study,[16] O_2 can be adsorbed molecularly across two adjacent coordinatively unsaturated vacancies. In the present study, O_2 is adsorbed molecularly across Ru_{cus} and Au as shown in Fig. 2(b). However, the bond length of O–Au is 2.626 Å, larger than that of O–Ru_{cus} at 1.927 Å. Additionally, the density plots of this configuration show that more charges transfer from Ru_{cus} to O^* than those from Au to O^*, which indicates that O is chemically adsorbed onto the Ru_{cus} stronger than onto the Au atom. The calculated Au–Ru_{cus}–O_2^* binding energy is −1.78 eV, larger than that of the adsorption at a single Ru_{cus} site. The features of O_2^* with a bond length of 1.31 Å and O–O stretching vibrational frequency of 1165.8 cm^{-1} are consistent with those of a superoxo-like O_2^- state. Figure 2(c) shows that the DFT-optimized O_2^* is bound at a single Au site. The O–O distance and stretching vibrational frequency are 1.267 Å and 1317.7 cm^{-1}, respectively. In this case, the O_2^* binding energy is only −0.44 eV and the density plot in Fig. 2(c) also illustrates that less charges transfer from Au to O_2, so this adsorption maybe physical adsorption.

Next, we consider O_2 adsorbed across adjacent vacant bridge A or B and Ru_{cus} or Au site as shown in Figs. 2(d) and 2(e). The binding energy of O_2^* adsorbed across O vacancy B and Ru_{cus} site is calculated to be −7.45 eV. Bader analysis indicates the bridge-$Ru_{cus}O_2^*$ to be reduced by 0.77 e^-. Furthermore, the O–O bond is lengthened to 1.413 Å, and O–O stretching vibrational frequency is red-shifted to 740.7 cm^{-1}.

These features are consistent with those of peroxide, which typically exhibits vibrational frequency closer to 850 cm^{-1} and a bond length of 1.49 Å. By contrast, the O_2^* adsorbed across O vacancy B and Au site is superoxo-like O_2^- with an O–O bond length of 1.33 Å and a vibrational frequency of 1078.7 cm^{-1}.

3.3. Dissociation of O_2^* and diffusion of O*

The minimum energy path from molecular O_2^* to dissociated oxygen O^*, calculated by CI-NEB method, is illustrated in Fig. 3. When the adsorbed O_2^* across vacant bridge B and Au sites dissociates into two O^* atoms, the O–O bond is stretched to 2.05 Å at the transition state (TS) as shown in Fig. 3(a). The calculated dissociation barrier for this case is 1.22 eV, much less than the desorption energy. By contrast, the dissociation barrier of O_2^* across vacant bridge A and Ru_{cus} is only 0.13 eV, which implies that dissociation is energetically more facile.

The dissociation of molecular O_2^* causes a single oxygen O^* to be adsorbed on Au or Ru_{cus} site. Furthermore, O^* can diffuse from Au to Ru_{cus} or in the reverse direction. The minimum energy paths of diffusion are calculated and shown in Figs. 3(c) and 3(d), respectively. The diffusion barrier of O^* from Au to Ru_{cus} is only 0.19 eV, much less than the diffusion barrier (2.84 eV) of O^* from Ru_{cus} to Au. The difference in diffusion barrier shows that O^* is easier to diffuse from Au to Ru_{cus}. Therefore, single oxygen O^* is adsorbed on the Ru_{cus} with greater probability.

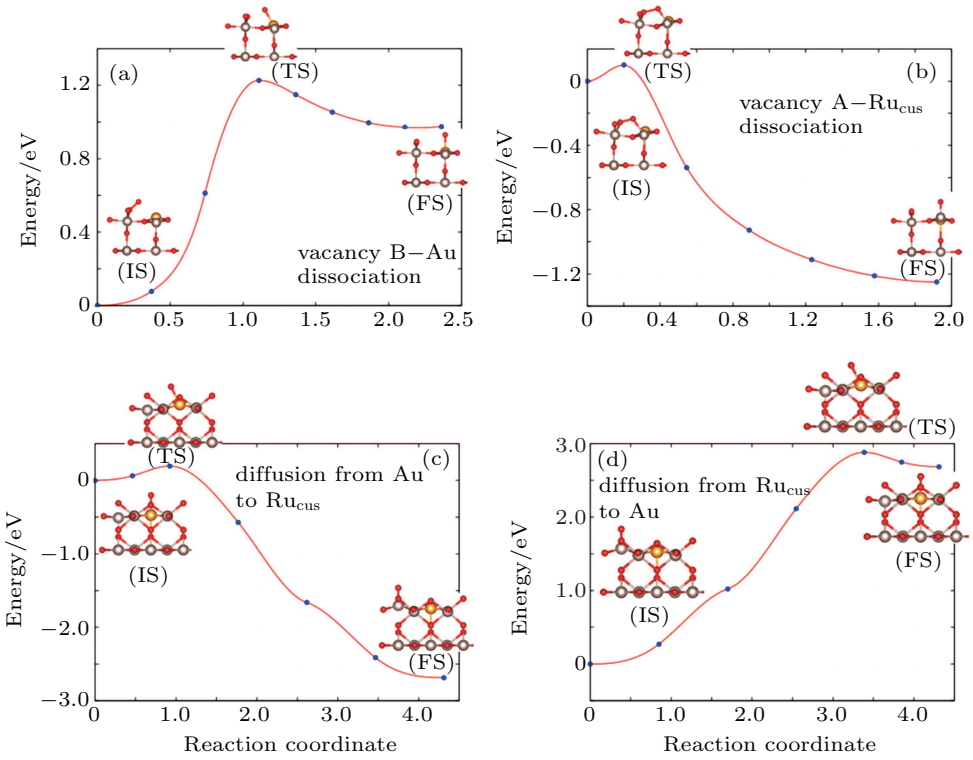


Fig. 3. Minimum energy path for O_2 dissociation at br vacancy B–Au and A–Ru_{cus} and diffusion of O^* between Ru_{cus} and Au. Cross-sectional structures are shown for initial state (IS), transition state, and final state (FS), with gray balls representing Ru, golden balls Au, and red balls oxygen.

3.4. CO oxidation on Au-doped RuO_2 (110) surface

The experimental study indicates that CO oxidizes readily into CO_2 on the RuO_2 (110) surface,[26–28] which is also corroborated by many theoretical investigations.[29,30] Previous studies show that CO is first adsorbed on the stoichiometric RuO_2 (110) surface, then reacts with the O-bridge atom. Finally, the CO_2 is desorbed with an O-bridge vacancy remaining. In the present study, two CO oxidation processes happening on the Au-doped RuO_2 (110) are considered. One is that the CO adsorbed on Au reacts with O-bridge to form CO_2, and the other is that the CO on Au combines with the O* adsorbed on the neighboring Ru_{cus}. The calculated relevant energy values and reaction paths are summarized in Fig. 4. There are two stable configurations for CO to be adsorbed on the Au atom. The molecular CO is adsorbed on the Au atom obliquely toward the O-bridge as shown in Fig. 4(a), which is chosen as an initial state to calculate the reaction path. Along the reaction coordinates, the C atoms from CO and the neighboring O-bridge move towards each other, reducing the distance from 3.57 Å to 1.98 Å at the transition state (TS). At the TS, the product-like OCO is formed with the $\angle OCO \approx 132.6°$. This conversion of CO to CO_2 has an energy barrier of 0.28 V, less than the value for the undoped case ($E_a = 0.7$ eV).[31] In addition, The reaction of CO adsorbed vertically on Au atom with O^* on the Ru_{cus} is considered as shown in Fig. 4(b). During the transition of the C atom from CO to O^*, the O and Ru_{cus}

together move close to the C atom. And the distance between C and O* is reduced from 3.38 Å to 1.64 Å at TS. This reaction is much more exothermic than reaction in Fig. 4(a).

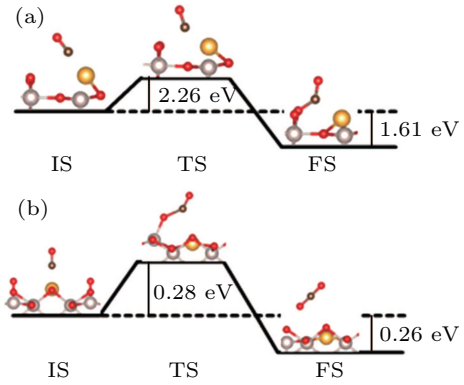


Fig. 4. Calculated potential energy diagram for CO oxidation on a gold atom doped in RuO_2 (110) surface.

4. Conclusions

The DFT calculation is carried out to describe the molecular oxygen adsorption and reaction chemistry of CO on the Au-doped RuO_2 (110) surface. The O_2 can be adsorbed on Ru_{cus}, Au, and oxygen bridge vacancies with different configurations. In comparison, the O_2 binding energy at the oxygen bridge vacancies is the largest, exceeding -6.98 eV, while the binding energy at the Au atom is only -0.44 eV. And it is found that the configurations can all dissociate at available neighboring vacant sites, which leaves a single O^* adsorbed at the Ru_{cus} and Au site. The calculation results indicate that the dissociated O^* is easier to diffuse from Au to Ru_{cus} site than from Ru_{cus} to Au. Finally, the CO reaction paths are obtained by DFT. The results show that the reaction energy barrier of CO adsorbed at Au with lattice oxygen decreases to 0.28 eV. However, the reaction of CO with O^* at Ru_{cus} site requires more energy.

References

[1] Henrich V E and Cox P A 1994 *The Surface Science of Metal Oxides* (Cambridge: Cambridge University Press)
[2] Noguera C 1994 *Physics and Chamistry at Oxide Surfaces Science* (Cambridge: Cambridge University Press)
[3] Over H, Kim Y C, Seisonen A P, Wendt S, Lundgren E, Schmid M, Varga P, Morgante A and Ertl G 2000 *Science* **287** 1474
[4] Fan C Y, Wang J, Jacobi K and Ertl G 2001 *J. Chem. Phys.* **114** 10058
[5] Wang J, Fan C Y, Jacobi K and Ertl G 2001 *Surf. Sci.* **481** 113
[6] Stampfl C, Schwegmann S, Over H, Scheffler M and Ertl G 1996 *Phys. Rev. Lett.* **77** 3371
[7] Monkhorst H J and Pack J D 1976 *Phys. Rev. B* **13** 5188
[8] Assmann J, Narkhede V, A Breuer N, Muhler M, Seitsonen A P, Knapp M, Crihan D, Farkas A, Mellau G and Over H 2008 *J. Phys. Condens. Matter.* **20** 184017
[9] Ertl G, Kno H and Weitkamp J 1997 *Handbook of Hetero-geneous Catalysis* (New York: Wiley)
[10] van Santen R and Neurock M 2006 *Molecular Heterogeneous Catalysis* (Weinheim: Wiley-VCH)
[11] Kim Y D, Seitsonen A P, Wendt S, Wang J, Fan C, Jacobi K, Over H and Ertl G 2001 *J. Phys. Chem. B* **105** 3752
[12] Rössler M, Günther S and Wintterlin J 2007 *J. Phys. Chem. C* **111** 2242
[13] Shapovalov V and Metiu H 2007 *J. Catal.* **245** 205
[14] Perdew J P, Burke K and Ernzerhof M 1996 *Phys. Rev. Lett.* **77** 3865
[15] Segall M D, Lindan P J D, Probert M J, Pickard C J, Hasnip P J, Clarck S J and Payne M C 2002 *J. Phys.: Condens. Matter* **14** 2717
[16] Wang H, Schneider W and Schnidt D 2009 *J. Phys. Chem. C* **113** 15266
[17] Henkelman G, Uberuaga B P and Jónsson H 2000 *J. Chem. Phys.* **113** 9901
[18] Henkelman G and Jónsson H 2000 *Chem. Phys.* **113** 9978
[19] Yang Z, Woo T K and Hermansson K 2004 *Chem. Phys. Lett.* **396** 384
[20] Sun Q, Rarsten K and Scheffler M 2004 *Phys. Rev. B* **70** 235402
[21] Boman C E 1970 *Acta Chem. Scand.* **24** 116
[22] O'Grady W E, Atanasoska L, Pollak F H and Park H L 1984 *J. Electroanal. Chem.* **178** 61
[23] Hong S and Rahman T S 2007 *J. Phys. Chem. C* **111** 12361
[24] Huber K P and Herzberg G 1079 *Molecular Spectra and Molecular Structure IV. Constants of Diatomic: Molicules* (New York: Van Nostrand Reinhold)
[25] Kung H 1989 *Transitition Metal Oxides: Surface Chemistry and Catalysis* (New York: Elsevier)
[26] Reuter K and Scheffler M 2003 *Phys. Rev. Lett.* **90** 046103
[27] Wang Y, Lafosse A and Jacobi K 2002 *J. Phys. Chem. B* **106** 5476
[28] Wang J, Fan C Y, Jacobi K and Ertl G 2002 *J. Chem. Phys. B* **106** 3422
[29] Reuter K and Scheffler M 2003 *Phys. Rev. Lett.* **90** 046103
[30] Reuter K, Frenkl D and Scheffler M 2004 *Phys. Rev. Lett.* **93** 116105
[31] Wendt S, Seitsonen A P and Over H 2003 *Catal. Today* **85** 167